Atmos. Chem. Phys., 14, 5617–5638, 2014
www.atmos-chem-phys.net/14/5617/2014/
doi:10.5194/acp-14-5617-2014

Atmospheric Chemistry and Physics
Open Access

Mapping Asian anthropogenic emissions of non-methane volatile organic compounds to multiple chemical mechanisms

M. Li[1,2], Q. Zhang[1], D. G. Streets[3], K. B. He[2], Y. F. Cheng[4], L. K. Emmons[5], H. Huo[6], S. C. Kang[2], Z. Lu[3], M. Shao[7], H. Su[4], X. Yu[8], and Y. Zhang[9]

[1]Ministry of Education Key Laboratory for Earth System Modeling, Center for Earth System Science, Tsinghua University, Beijing, China
[2]State Key Joint Laboratory of Environment Simulation and Pollution Control, School of Environment, Tsinghua University, Beijing, China
[3]Decision and Information Sciences Division, Argonne National Laboratory, Argonne, IL, USA
[4]Multiphase Chemistry Department, Max Planck Institute for Chemistry, Mainz, Germany
[5]Atmospheric Chemistry Division, National Center for Atmospheric Research, Boulder, CO, USA
[6]Institute of Energy, Environment and Economy, Tsinghua University, Beijing, China
[7]State Key Joint Laboratory of Environmental Simulation and Pollution Control, College of Environmental Sciences and Engineering, Peking University, Beijing, China
[8]Beijing Green Resource Research Co. Ltd., Beijing, China
[9]Department of Marine, Earth and Atmospheric Sciences, North Carolina State University, Raleigh, NC, USA

Correspondence to: Q. Zhang (qiangzhang@tsinghua.edu.cn)

Received: 25 November 2013 – Published in Atmos. Chem. Phys. Discuss.: 11 December 2013
Revised: 9 April 2014 – Accepted: 15 April 2014 – Published: 5 June 2014

Abstract. An accurate speciation mapping of non-methane volatile organic compounds (NMVOC) emissions has an important impact on the performance of chemical transport models (CTMs) in simulating ozone mixing ratios and secondary organic aerosols. Taking the INTEX-B Asian NMVOC emission inventory as the case, we developed an improved speciation framework to generate model-ready anthropogenic NMVOC emissions for various gas-phase chemical mechanisms commonly used in CTMs in this work, by using an explicit assignment approach and updated NMVOC profiles. NMVOC profiles were selected and aggregated from a wide range of new measurements and the SPECIATE database v.4.2. To reduce potential uncertainty from individual measurements, composite profiles were developed by grouping and averaging source profiles from the same category. The fractions of oxygenated volatile organic compounds (OVOC) were corrected during the compositing process for those profiles which used improper sampling and analyzing methods. Emissions of individual species were then lumped into species in different chemical mechanisms used in CTMs by applying mechanism-dependent species mapping tables, which overcomes the weakness of inaccurate mapping in previous studies. Emission estimates for individual NMVOC species differ between one and three orders of magnitude for some species when different sets of profiles are used, indicating that source profile is the most important source of uncertainties of individual species emissions. However, those differences are diminished in lumped species as a result of the lumping in the chemical mechanisms. Gridded emissions for eight chemical mechanisms at 30 min × 30 min resolution as well as the auxiliary data are available at http://mic.greenresource.cn/intex-b2006. The framework proposed in this work can be also used to develop speciated NMVOC emissions for other regions.

1 Introduction

Non-methane volatile organic compounds (NMVOCs) include a variety of chemical species that can be emitted from biomass burning, biogenic, and anthropogenic sources (Guenther et al., 2012; Piccot et al., 1992; van der Werf et

al., 2010). NMVOCs are of great concern because they play a key role in tropospheric chemistry as precursors of ozone and secondary organic aerosols (SOA) and many NMVOC species do damage to human health. NMVOCs differ significantly in their impacts on ozone and SOA formation, and these differences need to be represented appropriately in chemical transport models (CTMs). Such CTMs have been used to guide the development of emission control strategies by governmental agencies (e.g., US EPA, 2007; Wang et al., 2010; Xing et al., 2011), predict the effects of changes of emissions on the formation of ozone and SOA (e.g., Hogrefe et al., 2004; Y. Zhang et al., 2010, 2014), and study the sensitivity of the model predictions of pollutant concentrations to different gas-phase chemical mechanisms (e.g., Kim et al., 2011; Zhang et al., 2012).

In CTMs, atmospheric chemical reactions are usually characterized by a specific chemical mechanism, in which many individual NMVOC species are lumped together according to similarities in chemical structure or reactivity. The most commonly used chemical mechanisms in CTMs include the State Air Pollution Research Center 1999 version (SAPRC-99, Carter, 2000) and an updated version SAPRC-07 (Carter, 2010); Carbon Bond Mechanism version IV (CB-IV, Grey et al., 1989) and two variants with updates in reactions and related kinetic data including the Carbon Bond Mechanism version Z (CBMZ, Zaveri and Peters, 1999) and CB05 (Yarwood et al., 2005); as well as the second generation Regional Acid Deposition Model chemical mechanism (RADM2, Stockwell et al., 1990) and its variants with updates in reactions and related kinetic data including the Regional Atmospheric Chemistry Mechanism (RACM, Stockwell et al., 1997) and RACM2 (Goliff et al., 2013). This has been a challenge to map speciated NMVOC emissions data with organic compounds treated in different chemical mechanisms through a translation scheme from total NMVOC emissions to lumped, model-ready emissions. In the US National Emission Inventory system, The Sparse Matrix Operator Kernel Emissions (SMOKE) modeling system has been developed with the function of preparing model-ready NMVOC emissions as inputs for any chemical mechanisms (e.g., CB05, SAPRC-99, RADM2) used in CTMs. In the SMOKE model, total NMVOC emissions are first split into individual species by assigning appropriate source profiles from the US EPA's SPECIATE database (Hsu and Divita, 2009; Simon et al., 2010) using source classification codes, and then aggregated to lumped model species treated in different chemical mechanisms using corresponding mechanism-dependent mapping tables (Houyoux et al., 2000).

For the Asian region, although speciated NMVOC emissions have been estimated by various regional and global inventories (e.g., Klimont et al., 2002; Streets et al., 2003; Ohara et al, 2007; Bo et al., 2008; Wei et al., 2008), the interfaces between NMVOC emissions and CTMs remain underdeveloped. Table 1 summarizes the existing global and regional NMVOC emission inventories covering Asia. In addition to the known uncertainties in estimates for the total NMVOC emission budget, there are two other major weaknesses in Asian emission inventory data sets. First, most inventory data sets are not ready for model input. Although many global and regional inventories provide emissions of chemical species groups for Asia, based on reactivity and structure similarity (see Table 1), those species groups differ from lumped model species used in chemical mechanisms. The mapping process between species in inventories and models was usually performed by modelers without a standard procedure, which may lead to inaccuracies and introduce unpredictable uncertainties. This is especially true for a lumped-structure mechanism (e.g., carbon bond mechanism) where organics are grouped by chemical bond type (Fu et al., 2009). Second, recent local measurements on NMVOC source profiles have not been updated in most inventory studies. It is believed that NMVOC source profiles vary among regions worldwide as the consequence of differences in fuel quality and combustion conditions. For example, NMVOC composition from solvent use in China has been shown to be significantly different from those in the US (Yuan et al., 2010). Recognizing this problem, there are increasing numbers of measurements for local NMVOC source profiles in Asia. They cover many of the most important sources, such as residential fuel combustion (Tsai et al., 2003; Liu et al., 2008a; Wang et al., 2009), solvent use (Liu et al., 2008a; Yuan et al., 2010), petrochemical industry (Liu et al., 2008a), on-road transportation (Liu et al., 2008a; Lai et al., 2009), and fuel evaporation (Y. L. Zhang et al., 2013). However, only some of these locally measured profiles have been used in recent NMVOC emission inventories that covered part of China (Zheng et al., 2009) or the transportation sector in China (Cai and Xie, 2009). An updated Asian NMVOC emission database with state-of-the-art profiles is still missing.

In support of the US NASA Intercontinental Chemical Transport Experiment-Phase B (INTEX-B) mission, we developed an air pollutant emission inventory for Asia for the year 2006 (Zhang et al., 2009), including speciated NMVOC emissions as model-ready inputs for various chemical mechanisms (i.e., SAPRC-99, SAPRC-07, CB-IV, CB05, and RADM2), processed by an explicit speciation assignment approach. In the INTEX-B inventory, emissions for individual VOC species are first calculated for each source category by applying profiles from local measurements and the SPECIATE database, and individual species were lumped to emitted species in different chemical mechanisms by corresponding species mapping tables. The emissions data set for the SAPRC-99 mechanism is available to the public from http://mic.greenresource.cn/intex-b2006 and has been widely used in CTMs (e.g., Wang et al., 2011; Lin et al., 2012; Dong et al., 2013).

Although the step-by-step speciation process used in the INTEX-B inventory has provided model-ready NMVOC emission data to the community and reduced the

Table 1. NMVOC emission inventories covering Asian regions.

Inventory	Source[a]	Region	Year	Species included	Profiles used
EDGAR v2[b]	AN + BB	Global	1990	23 groups	Unknown
EDGAR v3[c] and v4[d]	AN + BB	Global	1970–2008	N/A	
POET[e]	AN + BB	Global	1990–2000	13 groups	Unknown
RETRO[f]	AN + BB	Global	1960–2000	22 groups	Unknown
Lamarque et al. (2010)	AN + BB	Global	1850–2000	22 groups	From RETRO
Klimont et al. (2002)	AN	China	1995	16 groups	SPECIATE
Streets et al. (2003)	AN + BB	Asia	2000	19 groups	SPECIATE
Ohara et al. (2007)[g]	AN + BB	Asia	1980–2003	N/A	
Kurokawa et al. (2013)	AN + BB	Asia	2000–2008	19 groups	From Streets et al. (2003)
Bo et al. (2008)	AN	China	1980–2005	N/A	
Wei et al. (2008)	AN	China	2005	40 groups including major individual active species	Local profiles + SPECIATE
Zheng et al. (2009)	AN + BG	PRD, China	2006	91 species from AN, and 30 species from BG	Local profiles + SPECIATE
Cai and Xie (2009)	Transportation	China	1980–2005	67 species	From literatures
This work	AN	Asia	2006	∼700 individual species; then mapping to emitting species of 8 chemical mechanisms	

[a] AN = anthropogenic; BB = biomass burning; BG = biogenic.
[b] available at http://www.pbl.nl/en/themasites/geia/emissions_data/nmvoc_groups/index.html.
[c] available at http://themasites.pbl.nl/tridion/en/themasites/edgar/emission_data/edgar32/index-2.html.
[d] available at http://edgar.jrc.ec.europa.eu/index.php; http://eccad.sedoo.fr.
[e] available at http://www.aero.jussieu.fr/projet/ACCENT/POET.php; http://eccad.sedoo.fr.
[f] available at http://retro.enes.org/data_emissions.shtml.
[g] not independent estimates. Data extrapolated from Klimont et al. (2002) and Streets et al. (2003).

uncertainties associated with inaccurate speciation mapping procedure, there remain many unresolved issues. Two major weaknesses are associated with profile selection and processing and need to be addressed. First, the INTEX-B profiles omit some important species, particularly oxygenated volatile organic compounds (OVOCs). OVOCs, which include alcohols, aldehydes, ketones and ethers, play a key role in atmospheric organic chemistry and many of them are known to have a detrimental effect on human health (Christian et al., 2004; Fu et al., 2008; Hopkins et al., 2003). The magnitude of OVOCs is significant and cannot be neglected for OVOC-rich emitting sources, such as biofuel burning and diesel vehicle exhaust (Andreae and Merlet, 2001; Schauer et al., 1999, 2001). Second, a single profile is assigned to each specific source, which may introduce inaccuracy into the speciation process due to the limitation of profiles (Cai and Xie, 2009; Reff et al., 2009). One limitation is that for sources containing multiple fuels and technologies, such as biofuel combustion, a single profile cannot represent the overall emission characteristics. On the other hand, the quality of profiles is difficult to quantify and may introduce unpredictable levels of uncertainty during profile selection.

In order to narrow the uncertainty from profile selection and processing mentioned above, we followed the speciation framework of the INTEX-B inventory but with necessary profile adjustments for OVOC-rich sources and the development of composite profiles in this work. We also evaluated the impact of profile update on the speciated emissions and ozone production, which is useful in understanding the uncertainties in emission speciation and determining the source of discrepancies between "bottom-up" emission inventories and "top-down" constraints (e.g., from in situ measurements and satellite observations).

This paper is organized as follows. Section 2 summarizes the methods and data that were used in this work and the INTEX-B inventory, including total NMVOC emissions, profile development, ozone formation potentials (OFPs) calculation, mechanism species mapping, and spatial allocation. Section 3 presents and compares the emissions of individual species and lumped mechanism species estimated in this work and the original INTEX-B inventory. In Sect. 4, the sensitivity of emissions and OFPs to profile selection is analyzed and the effects of updated profiles are assessed by comparing OFPs calculated from the two estimates. Prospectives for future work are discussed in Sect. 5.

2 Methodology and data

The general approach of speciation is to multiply total NMVOC emissions by a corresponding chemical speciation profile for each source type. Figure 1 presents the flow diagram of the methodology used in this work, as applied to the INTEX-B inventory. In this work, we start from total

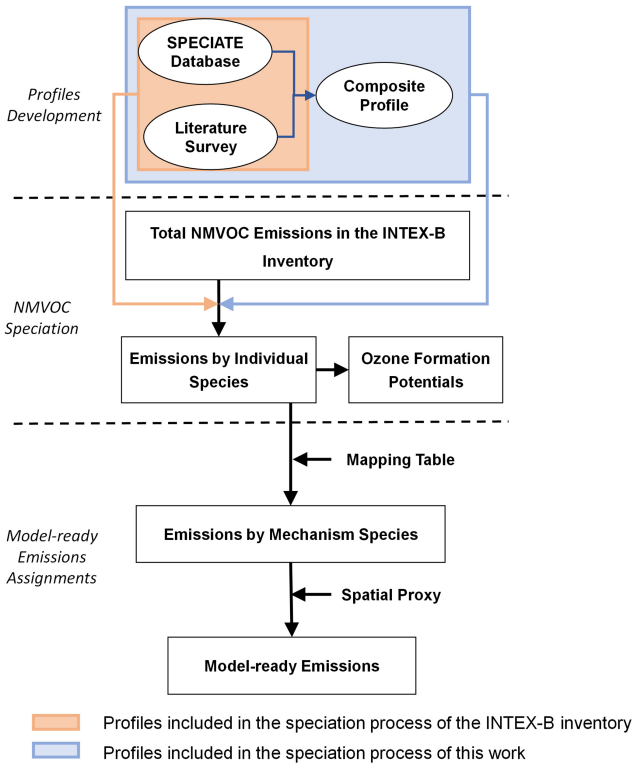

Figure 1. Schematic methodology of this study.

NMVOC emission estimates for 2006 in the INTEX-B Asian inventory (Zhang et al., 2009), select and aggregate profiles from both local measurements and the SPECIATE database v.4.2 (Hsu and Divita, 2009), and apply them to split total NMVOC into individual species. Compared to the INTEX-B inventory, the main difference of this work is the use of composite profiles. OFPs are calculated to evaluate the effect of profile update on ozone formation based on the speciated NMVOC emissions developed in this work. Individual species are lumped into model species of different mechanisms by specific mapping tables. Finally, gridded emissions are developed at 30 min × 30 min resolution using various spatial proxies.

2.1 NMVOC emissions in 2006 for Asia

Total NMVOC emissions were obtained from the 2006 Asian emission inventory for the NASA INTEX-B mission (Zhang et al., 2009). This inventory is an update of the TRACE-P Asian NMVOC inventory developed for an earlier NASA mission (Streets et al., 2003) with significant improvement for China using detailed activity data and local emission factors. The improved methodology for China led to a higher degree of source specificity in China than other Asian countries. To compile a speciated NMVOC emission data set with consistent and comparable methodology for all of Asia, a set of 55 source categories was aggregated by grouping similar source types for China and other Asian regions. Anthropogenic NMVOC emissions for 2006 for each source category are tabulated in Table S1. As estimated in the INTEX-B inventory, emissions from China (23.2 Tg) dominate total emissions in Asia (42 % of total), followed by Southeast Asia (14.1 Tg, 26 %) and India (10.8 Tg, 20 %).

Figure 2 presents the NMVOC emissions by eight sectors for China, other regions of East Asia, India, other regions of South Asia and Southeast Asia. For all of Asia, residential combustion, on-road transportation and industrial non-combustion contribute most to the total emissions, whereas the sector distributions vary significantly for different regions. For China, these three sectors share equally, whereas industrial non-combustion dominates the emissions for other East Asia. The shares of residential combustion and on-road transportation are significant both for India and other South Asia. For Southeast Asia, the emissions of total NMVOC are dominated by residential combustion and on-road transportation.

2.2 Development and assignment of source profiles

After classifying the INTEX-B total NMVOC emissions into grouped source categories, the next step is to assign or create a profile for each source. For a given source category, the profile development and assignment involve three steps: (1) search candidate profiles, both from the SPECIATE database v.4.2 and local measurements; (2) revise profiles that do not contain an OVOC contribution for OVOC-rich sources; and (3) construct "composite" profile if more than one profile is available.

The profiles are selected with the following steps. We first searched candidate profiles from SPECIATE database v.4.2 and a variety of literatures for each source category. The SPECIATE v.4.2 database provides the most comprehensive collection of available NMVOC profiles, containing more than 1600 source profiles from measurements mainly in the US (Simon et al., 2010). Because the fuel quality, combustion technology and emission regulations in Asia often differ significantly from those in the US, profiles taken from the SPECIATE database may not represent the chemical characteristics of sources accurately (Zheng et al., 2009). To develop a database of state-of-the-art profiles for Asia, local profiles for each emitting source type were gathered from the literature where available. As the numbers of locally measured profiles are still very limited, we include all available "local" profiles from literatures as candidate profiles. For those sources in which local profiles are available and we believe that there are significant differences between Asian and western countries, due to different technologies and/or legislations, only local profiles are used (e.g., solvent use). For sources in which similar technologies are used in Asian and western countries (e.g., boilers, vehicles), profiles from the SPECIATE database are also included. In order to reduce the uncertainties associated with profile selection in the original

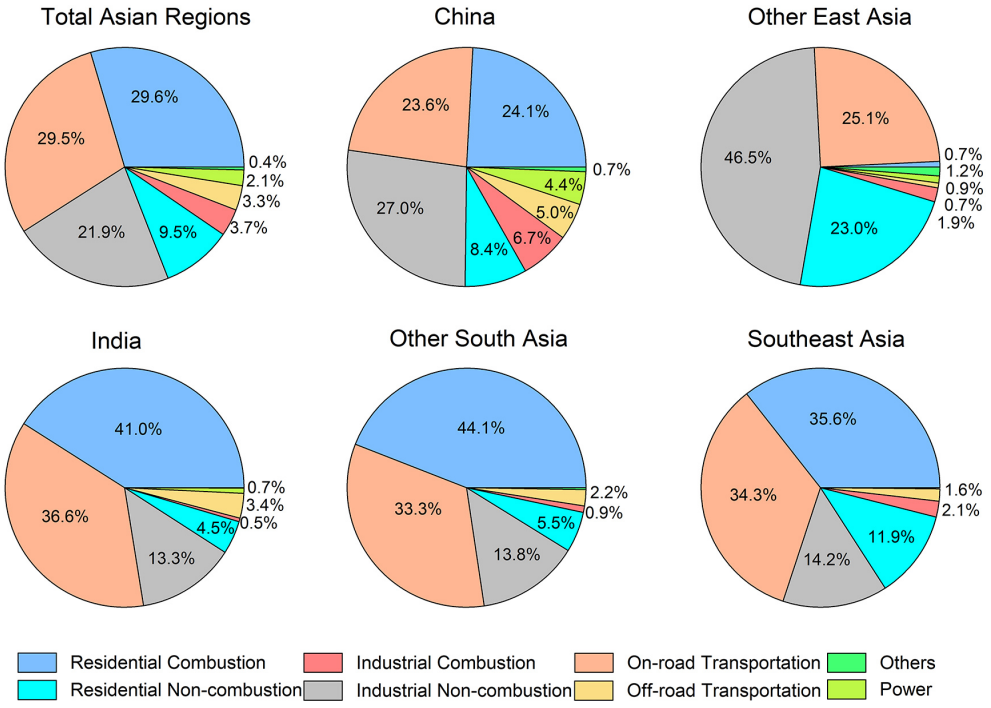

Figure 2. The 2006 NMVOC emissions by Asian regions in the INTEX-B inventory.

INTEX-B speciation process, as mentioned in Sect. 1, we take steps 2 and 3, respectively, to solve the "OVOC" and "single profile" issue. We identified the OVOC-rich sources and corrected the incomplete profiles which missed OVOC fraction. The "composite" profile for each source was finally developed with the same weighting factor for each individual candidate profile. The specific procedure is described below.

2.2.1 Inclusion of OVOC in profiles

From a comprehensive review of available profiles, we found that OVOCs contribute a large fraction of total NMVOC emissions from biofuel combustion and diesel vehicles (Schauer et al., 1999, 2001; Andreae and Merlet, 2001). However, OVOC fractions are missing in some profiles for these two sources due to sampling and analysis approaches (e.g., Liu et al., 2008a). Often, NMVOC samples were collected by canisters and then analyzed by gas chromatographic (GC) techniques, such as GC-mass spectrometry (GC-MS), GC-flame ionization detection (GC-FID), and GC-electron capture detection (GC-ECD) (Kelly et al., 1995). These techniques have proved to be accurate for determining the levels of hydrocarbons, but they are not suitable for analyzing carbonyl species because they cannot quantify unstable and "sticky" compounds accurately (Christian et al., 2004). Carbonyls are best analyzed by proton transfer mass spectrometry (PTR-MS) online monitoring (Christian et al., 2004) or collected by 2,4-dinitrophenylhydrazine (DNPH)-impregnated C18 cartridges and then analyzed by high-performance liquid chromatography with UV detection (HPLC/UV) (Schauer et al., 1999, 2001; Huang et al., 2011).

Until now, a standard protocol for NMVOC sampling and analysis is still not well developed. Many locally measured profiles used canisters to collect samples and GC techniques to analyze NMVOC species (e.g., Tsai et al., 2003; Liu et al., 2008a). In this work, we still include those profiles in the speciation process after correcting their OVOC fractions, as locally measured profiles are believed to better represent the real-world conditions. The general procedure of the revision is to append "OVOC" as a component to the original profile along with their percentage contribution calculated from profiles with OVOC measured for the same source. The fraction of each species except "OVOC" in the revised profile is calculated as

$$X_{\text{revised}}(i,j) = \frac{X_{\text{ori}}(i,j)}{\sum_j X_{\text{ori}}(i,j)} \times \left(1 - \overline{X_{\text{ovoc}}(i,j)}\right), \quad (1)$$

where i is the emitting source; j is the NMVOC species; $X_{\text{ori}}(i,j)$ and $X_{\text{revised}}(i,j)$ are the fractions of species j in the original and revised profiles of emission source i, respectively; X_{ovoc} is the proportion of OVOC for each selected profile that has OVOC measured for source i; and $\overline{X_{\text{ovoc}}}$ is the calculated mean of X_{ovoc}. The mass fraction of unspeciated "OVOC" in the revised profile is labeled with "missing value", not involved in the speciation process.

Figure 3 demonstrates inclusion of the missing OVOC fraction for the crop residue combustion profile measured by

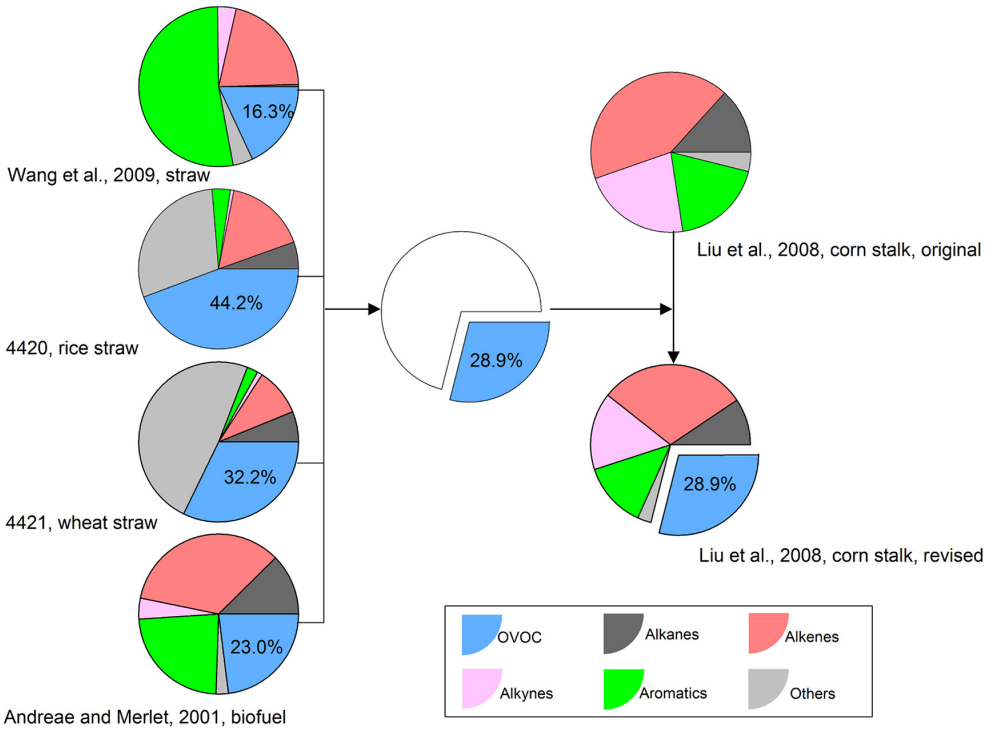

Figure 3. Inclusion of OVOC fraction for incomplete crop residue combustion profiles. The values 4420 and 4421 are the "P_NUMBER"s of profiles taken from the SPECIATE database developed by the US EPA.

Liu et al. (2008a). The average OVOC fraction, calculated as 28.9 % according to the four profiles that include OVOC (Andreae and Merlet, 2001; Wang et al., 2009; and profile no. 4420 and no. 4421 in SPECIATE v.4.2), is used to scale the original profile proportionally. Inclusion of OVOC fraction for diesel vehicle profiles is illustrated in Fig. S1. The revised profiles, along with other selected profiles, are then added to the profile database, ready for the next step of the speciation process.

2.2.2 Development of composite profiles

A"composite" profile is created for sources where multiple candidate profiles are available. For a given source category, species along with their mass fractions in each candidate profile are grouped and averaged, excluding missing values. It should be noted that the OVOC fractions in incomplete profiles are determined to be missing values, not involved in the calculation of average value. We choose median instead of mean as average to help mitigate possible large errors stemming from the presence of outlier samples and measurements (Reff et al., 2009). After the grouping and averaging process, the "composite" profile is scaled to 100 % proportionally. The grouping and averaging process can reduce the uncertainties of the empirical selection of profiles. However, it may introduce additional uncertainties from the assumption that each candidate profile for the same source is weighted equally.

Here we take the development of a composite profile for biofuel combustion as an example. Eleven profiles for crop residue and wood combustion were selected and processed into a composite profile, as listed from P1 to P11 in Fig. 4. The top 30 species and their corresponding fractions are presented, accounting for 84 % of the total mass in the composite profile. As shown in Fig. 4, measurements of species exhibit a large diversity among profiles. First, none of these species are contained in all profiles. In spite of the fact that species such as ethene, benzene and propane are included in most of the profiles, the fractions for some species are only included in one or two profiles (e.g., phenanthrene, glyoxal, and acetone), which introduces large uncertainties in the composite profile. Second, for specific species, fractions from different profiles vary significantly, revealing the discrepancies caused by different fuels and technologies of the emitting source and/or different samples and techniques used in the profile measurements. Thus, using a single profile will generate considerably different emissions for individual species, indicating the huge uncertainty associated with profile selection and application. The profile development method used in this work, by selecting and averaging multiple profiles, is an important way to reduce this uncertainty.

A complete list of profiles used in this work is presented in Table S1. The composited profiles developed in this work are available from the following website: http://mic.greenresource.cn/intex-b2006. The individual profiles

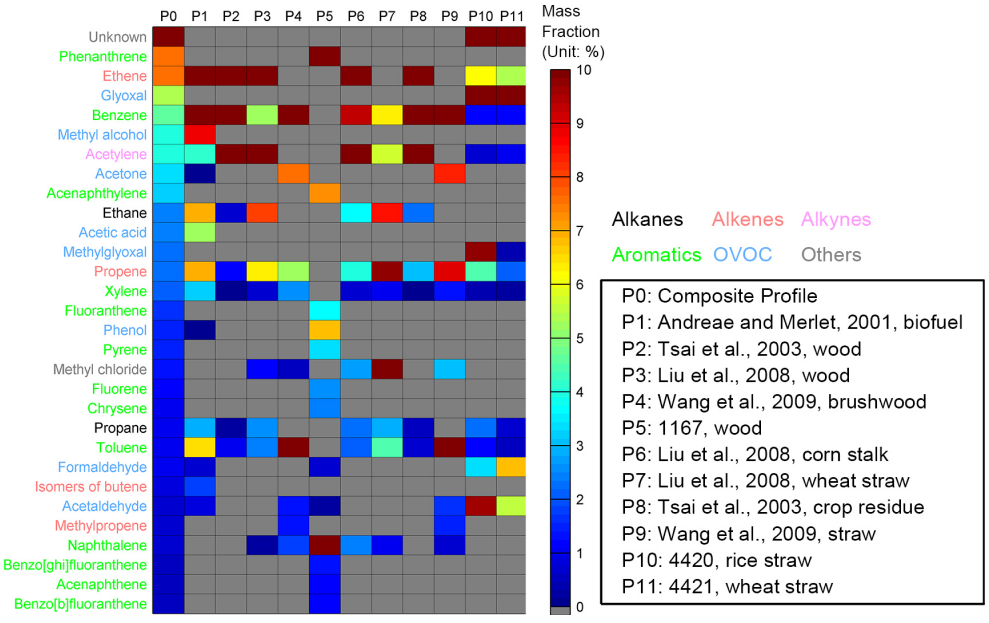

Figure 4. Mass fraction of major species in the profiles for the residential biofuel combustion. Top 30 species are presented and ranked decreasingly based on the mass fraction in the composite profile (P0). Gray grids indicate that mass fractions for these species are not included in the profile.

for diesel vehicles and the composite profile are illustrated in Fig. S2 as another example. After the profile-assignment speciation, region- and source-specific speciated NMVOC emissions for around 700 individual species are processed in this work, comprising the basic emission data set for lumping into different chemical mechanisms and OFP analysis.

2.3 Calculation of OFPs

The ozone reactivities for various NMVOC species differ significantly, which can be scaled by the maximum incremental reactivity (MIR) (Carter, 1994). OFP has been widely used in assessing the roles of NMVOC emissions in ozone formation and guiding the development of cost-effective ozone control measures (e.g., Song et al., 2007; Zheng et al., 2009), which can be estimated based on mass and MIR for each species. OFPs for individual species are calculated by multiplying emissions by corresponding MIR values:

$$\mathrm{OFP}(i,j,k) = \mathrm{EVOC}(i,k) \times X(i,j) \times \mathrm{MIR}(j), \quad (2)$$

where $\mathrm{OFP}(i,j,k)$ is the ozone formation potential of species j in region k, emitted from source i; $\mathrm{EVOC}(i,k)$ is the emission of total NMVOC for source i in region k; $\mathrm{X}(i,j)$ is the fraction of species j from the profile for source i, which is taken from the composite profiles developed in this work; $\mathrm{MIR}(j)$ is the maximum incremental reactivity scale for species j. OFPs by chemical groups and by sectors are calculated by summing up OFP values by corresponding individual species, to evaluate the ozone formation potentials of different chemical groups and sectors. It should be noted that species with no MIR values were ignored during the calculation of OFPs. This treatment will introduce uncertainties in evaluating the magnitude of OFPs but could be negligible when comparing the differences of identified compounds in this work.

2.4 Assignments for different chemical mechanisms

In atmospheric models, individual VOC emissions are usually assigned to "lumped" species in a simplified mechanism to balance the accuracy and computational efficiency, according to the similarities of their chemical reactivity. In this work, emission assignments for various chemical mechanisms are calculated by multiplying the emissions of individual species by species- and mechanism-specific conversion factors as follows:

$$\mathrm{EVOC}(i,k,m) = \sum_{j=1}^{n} \left[\frac{\mathrm{EVOC}(i,k) \times X(i,j)}{\mathrm{mol}(j)} \times C(j,m) \right], \quad (3)$$

where k is the region; m is species type in a mechanism; n represents the number of species emitted from source i. EVOC is the total NMVOC emissions; $X(i,j)$ is the mass fraction of species j to total NMVOC emissions for source i,which is obtained from the composite profiles; $\mathrm{mol}(j)$ is the mole weight of species j; and $C(j,m)$ is the conversion factor of species j for mechanism category m. In this work, the conversion factors were taken from the mechanism-dependent mapping tables developed by Carter (2013).

Table 2. Mapping table from SAPRC-99 species to GEOS-Chem species.

SAPRC-99	GEOS-Chem
ACET	ACET
CCHO	ALD2
ALK3 + ALK4 + ALK5	ALK4
ALK1	C2H6
ALK2	C3H8
HCHO	CH2O
MEK	MEK
OLE1 + OLE2	PRPE

Table 3. Mapping table from SAPRC-99 species to MOZART-4 species.

SAPRC-99	MOZART-4
ALK3[a] + ALK4 + ALK5	BIGALK
OLE2	BIGENE
ARO1 + ARO2	TOLUENE
OLE1	C3H6
ALK2	C3H8
ALK1	C2H6
ETHE	C2H4
MEK + PRD2	MEK
HCHO	CH2O
CCHO	CH3CHO
ACET	CH3COCH3
MEOH	CH3OH
not available	C2H5OH[b]

[a] Ethyl alcohol is removed from ALK3 when mapping to BIGALK.
[b] Taken from ethyl alcohol emissions.

Table 4. Spatial proxies used in this work.

Source category	Spatial proxies
Large power plants (>300 MW)	Location
Small power plants (< 300 MW)	Total population
Industry combustion	Urban population
Residential boilers	Urban population
Residential biofuel	Rural population
On-road transportation	Road network
Off-road transportation	Rural population
All other sources	Total population

For some profiles, a fraction of total NMVOC is assigned as "unknown" or "undefined" species, which probably reflects the unidentified fraction arising from the limitation of the analysis technique (Schauer et al., 1999). In this work, we treated the "unknown" species as a single species during the composite profile development and then assigned emissions from "unknown" species mainly into ALK5, NROG, OLE1, ARO1, and ARO2 in the SAPRC-99 mechanism and PAR, UNR, OLE, TOL, XYL, and ALDX in CB05, according to Carter (2013). However, the "unknown" species is not included in the OFP calculation, as its maximum incremental reactivity is undefined.

Emissions for six chemical mechanisms are calculated in this work based on the availability of mapping tables in Carter (2013): CB-IV, CB05, SAPRC-99, SAPRC-07, RADM2 and RACM2. These mapping tables are available at http://www.engr.ucr.edu/~carter/emitdb/. In these tables, each individual organic compound is assigned with conversion factors to mechanism species according to its carbon bond (for CBIV and CB05) and chemical group (for SAPRC-99, SAPRC-07, RADM2, and RACM2); hence it provides a consistent way of species mapping for different chemical mechanisms. To our knowledge, this is the most accurate chemical mapping approach in the community, which has been used in processing US emission inventories. We also calculated emissions for two global models, GEOS-Chem and MOZART-4, by lumping SAPRC-99 species to emission species in those two global models. The mapping tables from SAPRC-99 species to GEOS-Chem and MOZART-4 species are presented in Tables 2 and 3 and the abbreviations of those species are provided in Tables A1–A4.

2.5 Spatial allocation

Emissions are gridded for CTMs and aggregated into four sectors (power, industry, residential and transportation), both by individual species and by chemical mechanisms. We followed the top-down approach used in the INTEX-B inventory (Zhang et al., 2009) to distribute country- or provincial-level emissions to grids using various spatial proxies at 1 km × 1 km resolution (Streets et al., 2003; Woo et al., 2003). Spatial proxies used in this work include: total population data extracted from LandScan Global Population Dataset developed by Oak Ridge National Laboratory (ORNL, 2004), urban and rural population data developed from partitioning total population using urban land cover from LandScan 2000 database (ORNL, 2002), and road networks from the Digital Chart of the World (DCW, 1993).

Table 4 listed the spatial proxies used in this work. All power generation units with capacity larger than 300 MW in China are identified as large point sources, while other plants are treated as area sources and distributed by total population. Urban population was used for distributing emissions from industrial combustion, residential coal-fired boilers; rural population was used for residential biofuel combustion and off-road transportation; road networks were used for on-road transportation emissions; and total population was used for all other area sources. The final gridded emissions were aggregated to 30 min × 30 min resolution.

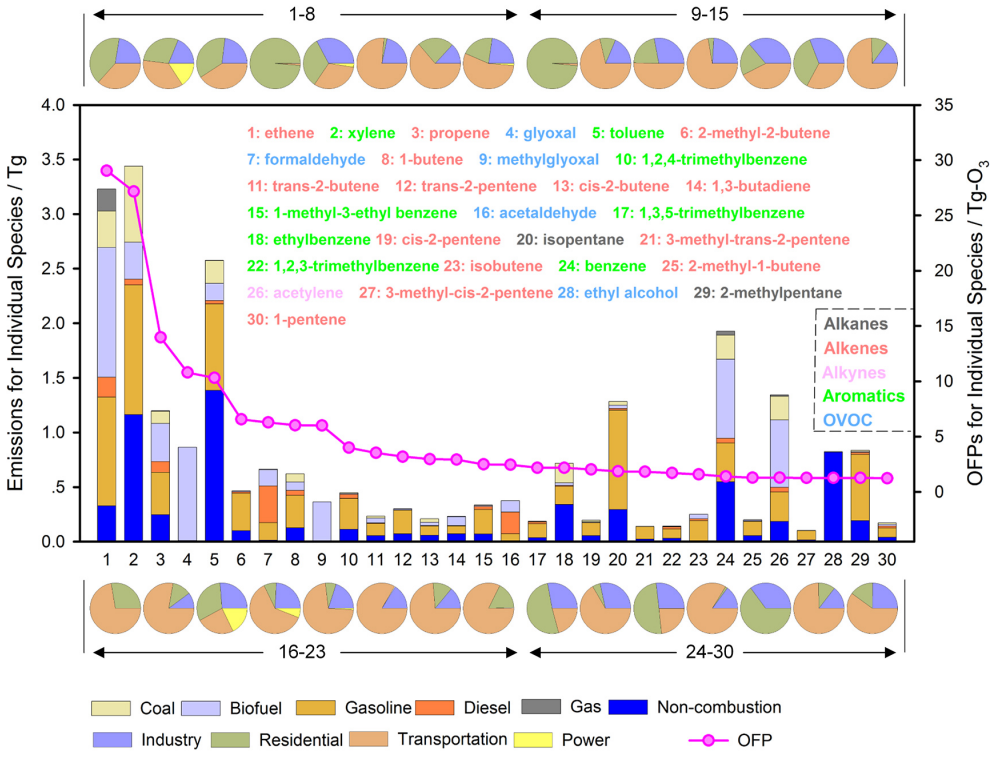

Figure 5. Emissions by individual NMVOC species and corresponding OFPs.

3 Results

3.1 Speciated NMVOC Emissions by individual species

Using the approaches described in Sect. 2, emissions of ~700 individual NMVOC species for Asia are estimated for the year 2006. Figure 5 presents emissions of the 30 species with the highest OFPs for the whole Asian region. These top 30 species contributed 44 % to total Asian anthropogenic NMVOC emissions and 82 % to total OFPs. For species with small emissions, the emission estimates have high uncertainty due to the inaccuracy of the emission profiles and omission of minor emitting source types.

As shown in Fig. 5, the order of OFPs of the top 30 species differs significantly from that of emissions (by mass), which is attributed to the variation of chemical reactivity of species, scaled by MIR in this work. Emphasis is placed on OVOCs and alkenes with high MIRs and relatively high contribution to OFPs. It is interesting to notice that some OVOCs, such as glyoxal and methylglyoxal, are determined to have high OFPs but relatively low-emission estimates, due to their high-reactivity scales. Alkanes and some aromatics (e.g., benzene) tend to be less chemically reactive in the atmosphere and have lower contribution to OFPs compared to their emissions.

Figure 5 also shows the distribution of individual species emissions among major contributing source types (by fuel type and by sector). Gasoline and biofuel combustion are two common significant contributing sources for most species, with the exception of a high proportion of contribution from non-combustion sources for aromatics (e.g., 34 % for xylene, 54 % for toluene). Ethene is the largest contributor to ozone formation potential (29.0 Tg-O_3) with the second highest emissions (3.2 Tg), coming mainly from biofuel combustion (1.2 Tg, 38 % of total), gasoline combustion (1.0 Tg, 32 %), coal combustion (0.3 Tg, 10 %), and non-combustion sources (0.3 Tg, 10 %). Alkenes other than ethene such as propene, 2-methyl-2-butene, 1-butene also have significant contributions to OFPs. Propene is the third largest contributor to ozone formation, having similar distribution by fuel and sector as ethene. Important aromatic ozone precursors include xylenes, toluene, and 1,2,4-trimethylbenzene. We estimate that xylene emissions in Asia in 2006 were 3.4 Tg (27.2 Tg-O_3 ozone formation potential), ranking first in terms of magnitude of emissions and second in terms of OFPs.

As shown in Fig. 5, glyoxal, formaldehyde, methylglyoxal, acetaldehyde, and ethyl alcohol are OVOC species with remarkable contributions to anthropogenic OFPs over Asia. Some of OVOCs (e.g., glyoxal and methylglyoxal) also have important contributions to SOA formation through aqueous-phase reactions in aerosols and clouds (Carlton et al., 2007; Ervens and Volkamer, 2010). In this work, primary glyoxal and methylglyoxal are mostly emitted from biofuel combustion. However, it should be noted that incomplete profiles for other sources resulting from inappropriate sampling and

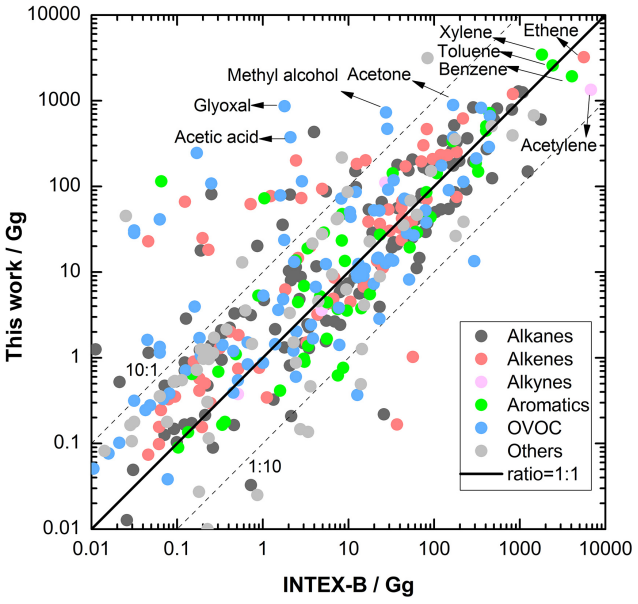

Figure 6. Comparison of this work and the INTEX-B inventory by individual species.

analysis methods are a potential source of high uncertainty; newly measured profiles may provide additional sources of these OVOC species in the future.

Figure 6 compares the emissions of individual species estimated in this work and the original INTEX-B emission inventory, based on the same total NMVOC emission estimates. A total of 425 species were presented in Fig. 6, covering the species with annual emissions larger than 10 Mg in two inventories. Large differences are observed, having a general pattern of more OVOC and alkenes emissions estimated from this work than in the original INTEX-B inventory. For 132 species (31 % of total), the differences between the two estimates were within 100 %, while emission estimates for 60 species (14 % of total) differ by one order of magnitude or more, implying that large uncertainties are introduced from NMVOC source profiles. Considering that the uncertainties associated with activity rates and total NMVOC emission factors are usually less than 100 % (Zhao et al., 2011), the source profiles could be recognized as the most important source of uncertainties in emission estimates for individual NMVOC species. This, in turn, has significant implications for the ability of CTMs to reliably model the oxidizing nature of the Asian atmosphere.

Compared to the original INTEX-B inventory, this work estimated much lower emissions for acetylene, but higher emissions for xylene and glyoxal (as shown in Fig. S3). The significant decrease of acetylene emissions and increase of xylene and glyoxal emissions are mainly due to the change of residential biofuel combustion profile. As can be seen from Fig. 4, the profile used in the original INTEX-B inventory is taken from Tsai et al. (2003) (P2 and P8), which contains high-mass fraction of acetylene (27.4 % for P2 and 27.0 % for P8, respectively) in contrast to the composite profile.

For species like ethene, benzene and acetylene, emissions are lower than in the INTEX-B inventory; whereas propene, xylene, glyoxal, acetone, and methyl alcohol emissions are higher. Because alkenes, aromatics and OVOC are reactive precursors for ozone and SOA formation, these differences in emissions may lead to enhancements in OFPs and ozone and SOA concentrations simulated by CTMs. The impact of emission differences from the speciation process on OFPs will be quantified and discussed in the next section.

Figure 7 shows the spatial distribution of toluene emissions in 2006 at 30 min × 30 min horizontal resolution. Gridded emissions for ∼700 individual species at the same resolution are all developed following the methodologies described in Sect. 2.5 and are available by request. These data sets would be useful for comparing with in situ measurements and identifying possible sources of uncertainties in emission inventories (e.g., Wang et al., 2013). However, as emissions of some species may differ by 1–3 orders of magnitude when assigning different sets of profiles, these data sets should be used with caution in interpreting the discrepancy between observations and NMVOC emissions, because the discrepancy may be attributed to uncertainties in the profiles rather than in total NMVOC emissions.

3.2 Speciated NMVOC emissions by chemical groups

Figures 8 and 9 present 2006 NMVOC emissions in Asia by chemical groups estimated in this work. We estimate that alkenes accounted for the largest share of Asian total NMVOC emissions in 2006 (240 Gmole (10^9 mole), 30 % of total), followed by alkanes (191 Gmole, 24 %), OVOCs (155 Gmole, 17 %), aromatics (114 Gmole, 14 %), and alkynes (56 Gmole, 7 %). The shares from alkanes and aromatics are larger in Japan and South Korea (other East Asia) than in other regions, reflecting the significant contribution from the industrial sector in the two countries.

We also compared emissions estimated in this work with the original INTEX-B inventory by chemical groups in Figs. 8 and 9. In contrast to the large differences in emission estimates for individual species, the discrepancies are reduced greatly after grouping individual species into similar chemical functional groups. The emission differences of alkanes, alkenes, and aromatics are within 5 % between the original INTEX-B inventory and this work, while significant differences were still found for alkynes and OVOC emissions. A large increase compared to the original INTEX-B inventory is observed for OVOC emissions, from 53 Gmole yr^{-1} to 155 Gmole yr^{-1}, in contrast to the decrease of alkynes emissions from 261 Gmole yr^{-1} to 56 Gmole yr^{-1}. Similar differences are found in all Asian regions except other East Asia, where the two estimates show similar distributions among chemical groups.

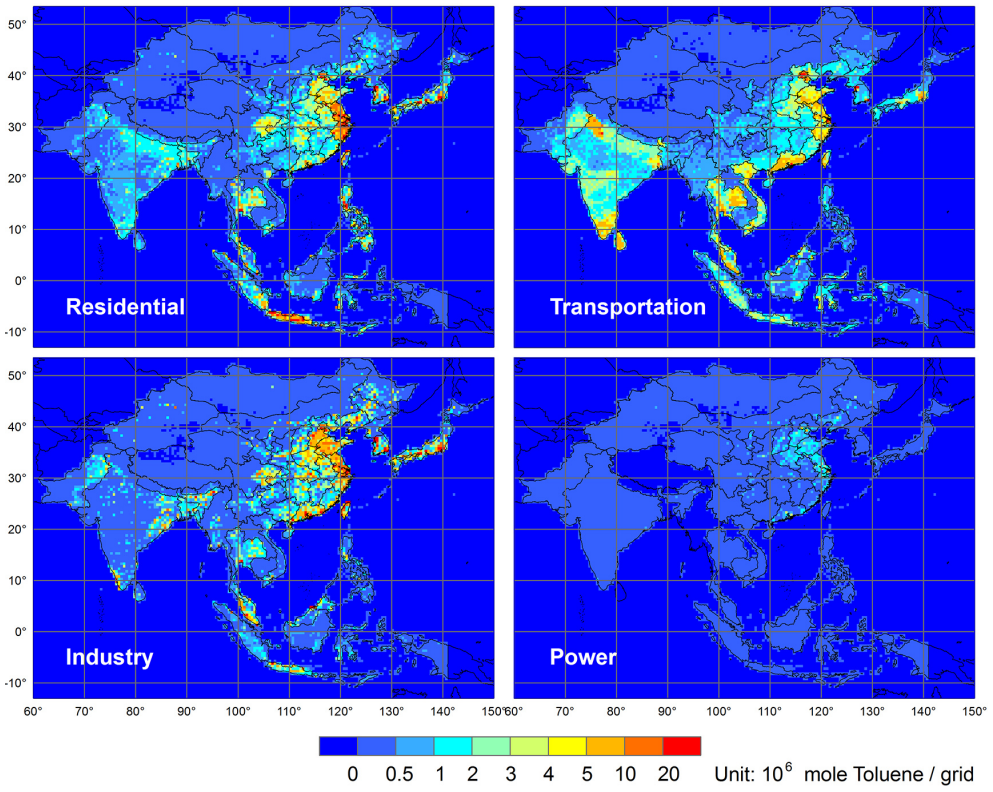

Figure 7. Emission distribution of toluene by sector at 30 min × 30 min resolution (unit: 10^6 mole yr^{-1} per grid).

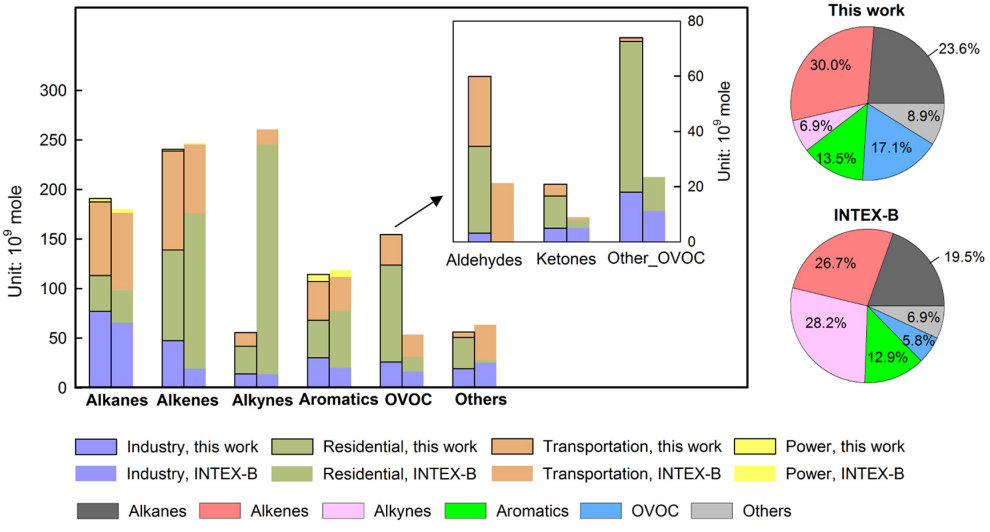

Figure 8. Asian anthropogenic NMVOC emissions in 2006 by chemical groups.

The dramatic increase for OVOC emissions and decrease for alkynes emissions is dominated by the residential sector, mainly due to the creation and application of the "composite" profile for biofuel combustion. The P2 and P8 profiles (both measured by Tsai et al., 2003) that were used in the original INTEX-B speciation process are incomplete profiles that miss the contributions from OVOCs. The increase of OVOC emissions is due to the inclusion of the OVOC fraction in the "composite" profile. Compared to P2 and P8, other candidate profiles have a much lower contribution from acetylene (see Fig. 4), leading to the lower share of alkynes in the "composite" profile used in this work. The inclusion of OVOC in incomplete profiles further decreases the contributions for

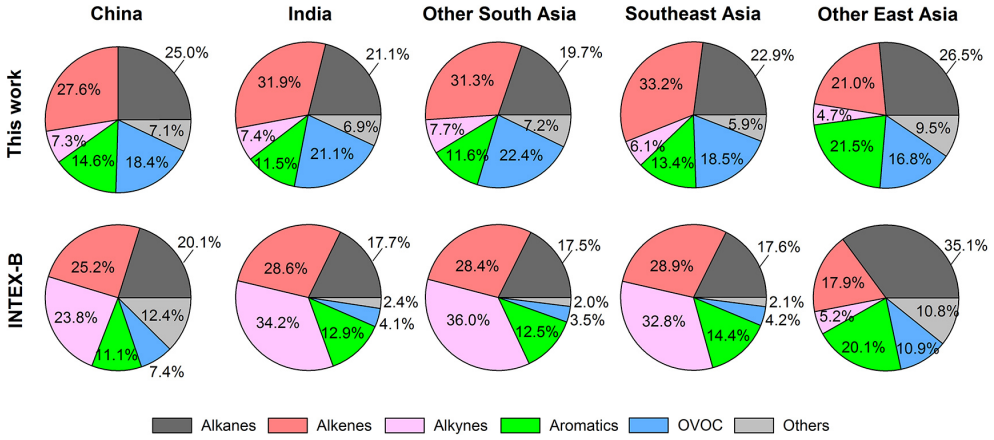

Figure 9. Distribution of anthropogenic NMVOC emissions in 2006 among different chemical groups for Asia regions.

non-OVOC species, which also contribute to the differences in alkyne contributions.

3.3 Model-ready emissions

One of the key objectives of this study is to develop model-ready NMVOC emission data sets for Asian anthropogenic sources as the emission inputs for CTMs. In this work, model-ready emissions for eight chemical mechanisms were developed: CB-IV, CB05, SAPRC-99, SAPRC-07, RADM2, RACM2, GEOS-Chem, and MOZART-4. Emissions for the GEOS-Chem model and MOZART-4 model were converted from SAPRC-99 emissions using the species mapping tables presented in Tables 2 and 3. Figure 10 illustrates the 2006 Asian anthropogenic NMVOC emissions lumped by SAPRC-99 and CB05 species. Emissions are then distributed by various spatial proxies following the approaches described in Sect. 2.5 and aggregated at 30 min × 30 min resolution. Gridded emissions for the eight chemical mechanisms mentioned above are all available from our website (http://mic.greenresource.cn/intex-b2006). Gridded emissions are provided for four sectors: power plants, industry, residential, and transportation. Those data can be used directly as model inputs without further species mapping. As an example, Fig. 11 presents the map of OLE1 (a SAPRC-99 species) emissions by sector covering all regions included in this work, showing a broad spatial distribution among residential, transportation and industry sectors.

As individual species are usually highly lumped in CTMs, it is important to investigate how the speciation process impacts emissions in lumped species in different mechanisms. In Fig. 10, we compare the speciated emissions assignments by the SAPRC-99 and CB05 mechanisms, both in the INTEX-B inventory and this study. The differences in lumped species emissions between the original INTEX-B inventory and this work are much smaller compared to individual species, indicating that the uncertainties associated with profile selection and processing are diminished as a result of the lumping in the chemical mechanisms.

However, there are still significant differences between the two estimates. For SAPRC-99 species, sharp increases of OVOC and ARO2 emissions from the residential sector are found, contrasting with a decrease of ETHE (ethene) and ALK2 (primarily propane and acetylene) emissions for the same sector. OLE1 and OLE2 emissions from the transportation sector are larger in this work, contributing to the differences in the two estimates for those two species. These differences are mainly attributed to the updated profiles of biofuel combustion and on-road vehicles. The differences between the two estimates by CB05 species show similar patterns as the SAPRC-99 species (although this was represented in different lumping species), while PAR emissions agree well between the two estimates, due to a high degree of lumping.

Figure 12 further presents emissions by SAPRC-99 species for each Asian region and compares with the original INTEX-B estimates. As the emission characteristics for other South Asia are very close to India, we present emissions of South Asia as a whole. For South Asia and Southeast Asia, where emissions are dominated by the residential sector, the two estimates differ significantly in OVOC, ALK2, and ETHE emissions due to updates of profiles in residential and transportation sector, as discussed above. For other East Asia, the differences between the two estimates are smaller, because the NMVOC emissions are dominated by the industrial sector in which similar profiles were used.

4 Impacts of profile development on ozone production

4.1 Ozone formation potentials (OFPs)

Given the fact that emission estimates of individual NMVOC emissions in Asia are heavily influenced by source profiles, it is important to understand how the variations in emission estimates then impact the prediction of ozone production.

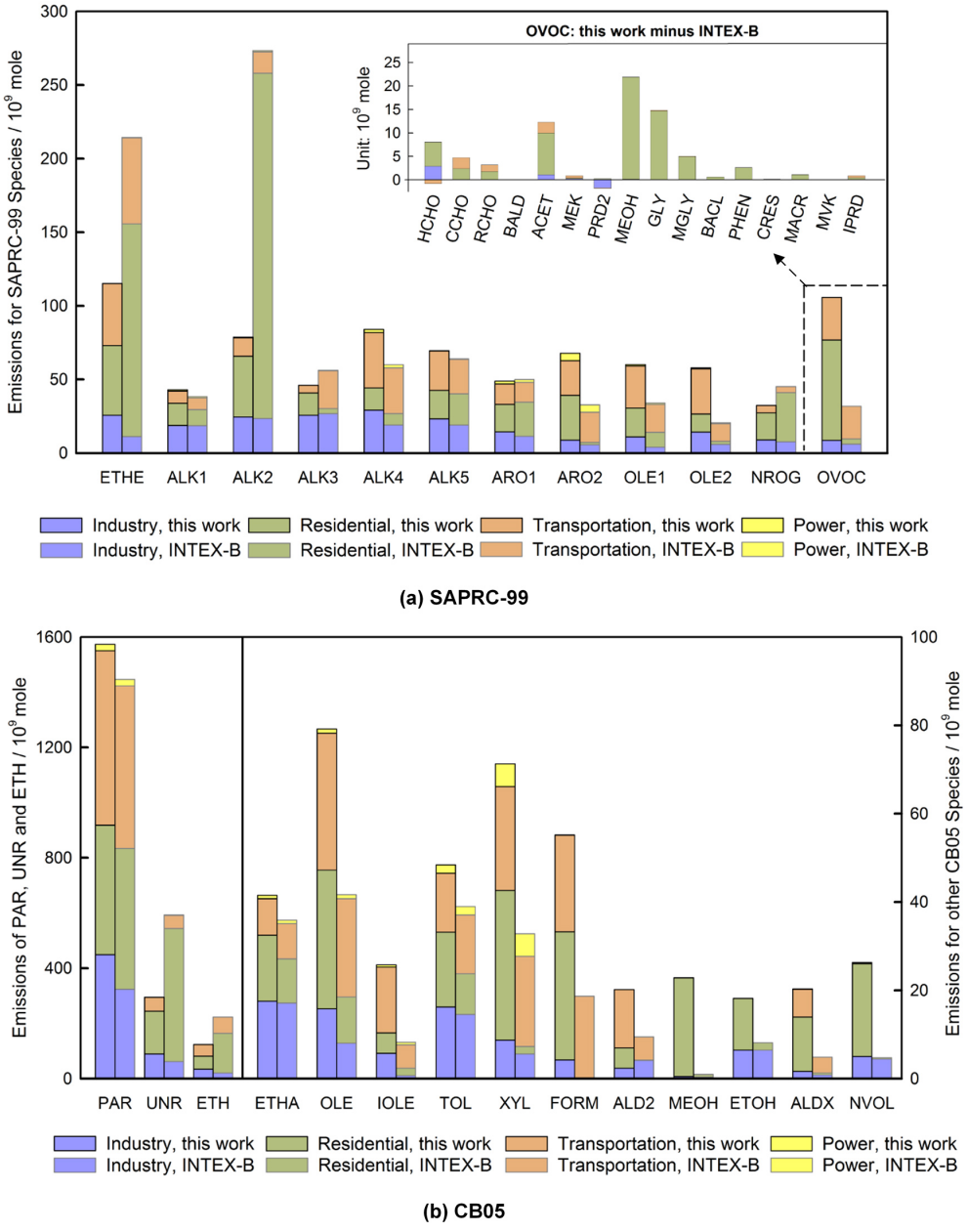

Figure 10. 2006 Asian anthropogenic NMVOC emissions by SAPRC-99 **(a)** and CB05 **(b)** species. An explanation of the abbreviations of SAPRC-99 and CB05 emitting species are presented in Tables A1 and A2.

Based on the emissions by individual species and corresponding MIR, OFPs of Asian anthropogenic NMVOC emissions in 2006 are calculated by sector and chemical groups, as presented in Fig. 13.

The total OFPs of 2006 Asian anthropogenic NMVOC emissions calculated in this work are 195 Tg-O_3, 33 % higher than the OFPs from the original INTEX-B inventory, indicating that the compilation of NMVOC source profiles can significantly impact estimates of ozone production. In this work, we estimated that alkenes have the largest contribution to total OFPs (46 %), followed by aromatics (28 %), OVOC (18 %), alkanes (7 %), and alkynes (1 %). Alkenes and OVOCs have larger contributions to total OFPs than to total emissions, while alkanes and alkynes have smaller contributions to OFPs due to their relatively low MIR.

Compared to the INTEX-B inventory, higher OFP contributions from alkenes, aromatics, and OVCs are estimated. Higher OFPs from alkenes are mainly because the locally measured profiles included for the transportation and industrial sectors have higher proportions of propene and butenes, which have larger MIR than ethene. Ethene contributes 34 % to the total OFPs of alkenes in our new estimates, much lower

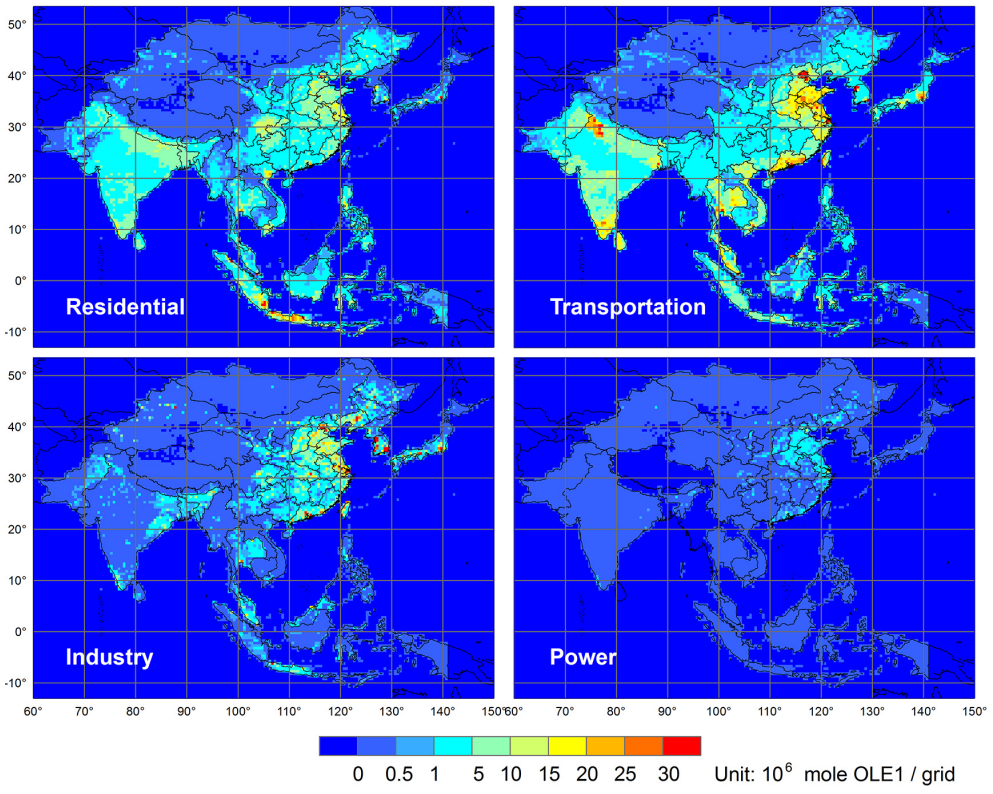

Figure 11. Emission distribution at 30 min × 30 min resolution of OLE1, SAPRC-99 species.

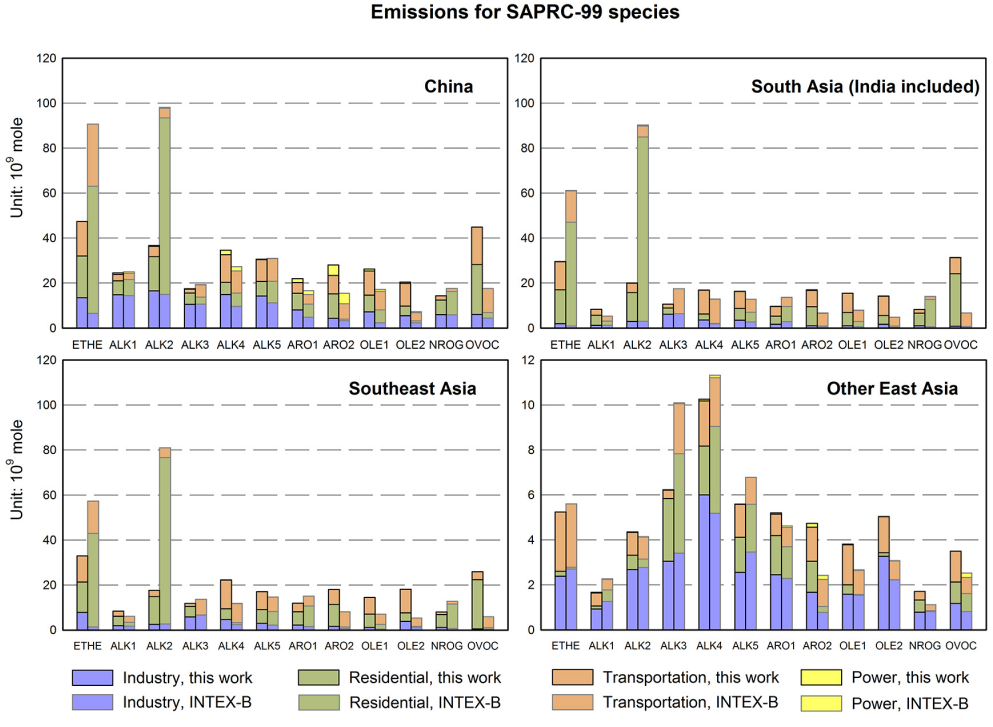

Figure 12. The 2006 Asian emissions for SAPRC-99 mechanism species by regions.

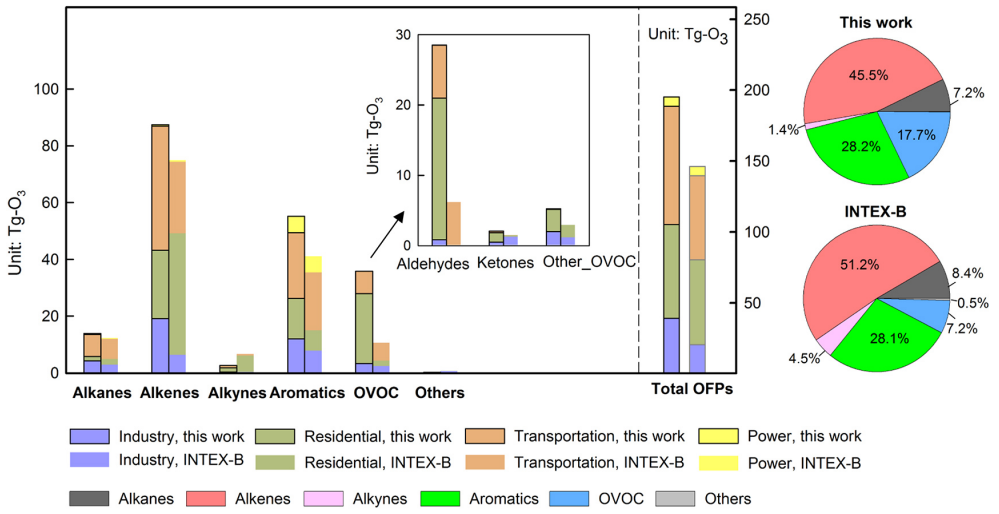

Figure 13. Ozone formation potentials (OFPs) of Asian anthropogenic NMVOC emissions in 2006 by chemical groups.

than the 58 % in the original INTEX-B inventory. For aromatics, the emission increase from aromatics other than benzene, especially xylenes with high-ozone reactivity, accounts for the increase of OFP. The increase in the OFP contribution from OVOCs can be attributed to higher estimates of aldehyde emissions from the residential sector. Note that total OFPs from the residential sector are almost the same between the two estimates, which is mainly due to an offsetting of the increase in emissions of OVOC by a decrease in emissions of alkenes.

4.2 Sensitivity analysis of individual profiles

Since significant differences in emissions and OFPs are observed between the original INTEX-B inventory and this work, which is attributed to the update of profile selection and compilation, it is worth examining the sensitivity of individual profiles to emission estimates and OFPs. From the analysis presented above, we found that the profiles for biofuel combustion and on-road vehicles contributed significantly to those differences. In this work, 11 biomass burning profiles covering different fuel types and combustion conditions are used for compiling the "composite" profile of biofuel combustion, as shown in Fig. 4. Emissions by individual species vary significantly among these 11 profiles, which is partly due to the variation in fuel and combustion types. When developing the Asian NMVOC emission inventory, such variations were ignored by treating biofuel combustion as a single source category, due to the lack of detailed statistics on fuel types and combustion conditions.

Based on the concept of MIR for individual species, we evaluate the ozone reactivity scale for each profile by calculating OFPs per unit NMVOC emission, as shown in Fig. 14, to determine the sensitivity of OFPs to source profiles. The profiles from Andreae and Merlet (2001) (P1) and no. 4420

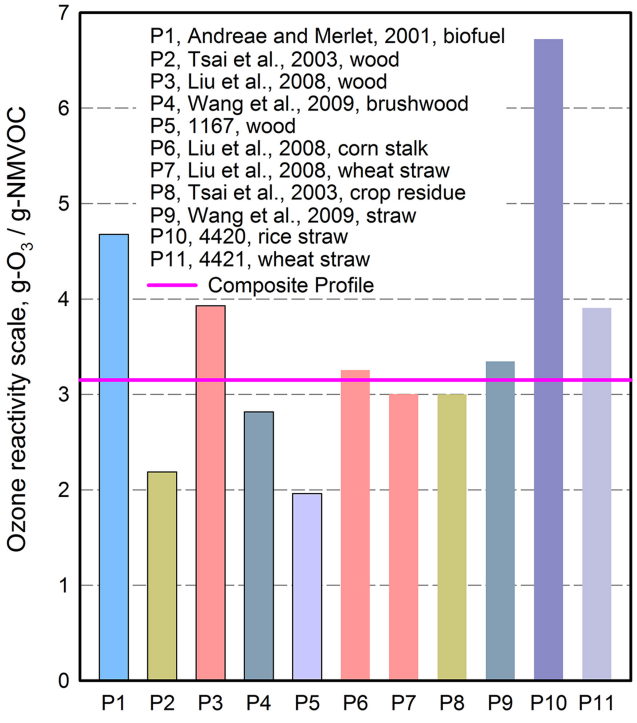

Figure 14. Sensitivity of OFPs to profile selection for the residential biofuel combustion.

from the SPECIATE database v.4.2 (P10) tend to produce more ozone when used in the speciation, because of the high fractions of alkenes and OVOC, respectively. Since the OVOC fraction is relatively high in P10, contributions to ozone formation from OVOC might be overestimated if only P10 was used for biomass burning, whereas they may be underestimated by using P2, P3, P6 or P7 (Tsai et al., 2003; Liu et al., 2008a), which have no OVOC measured. The

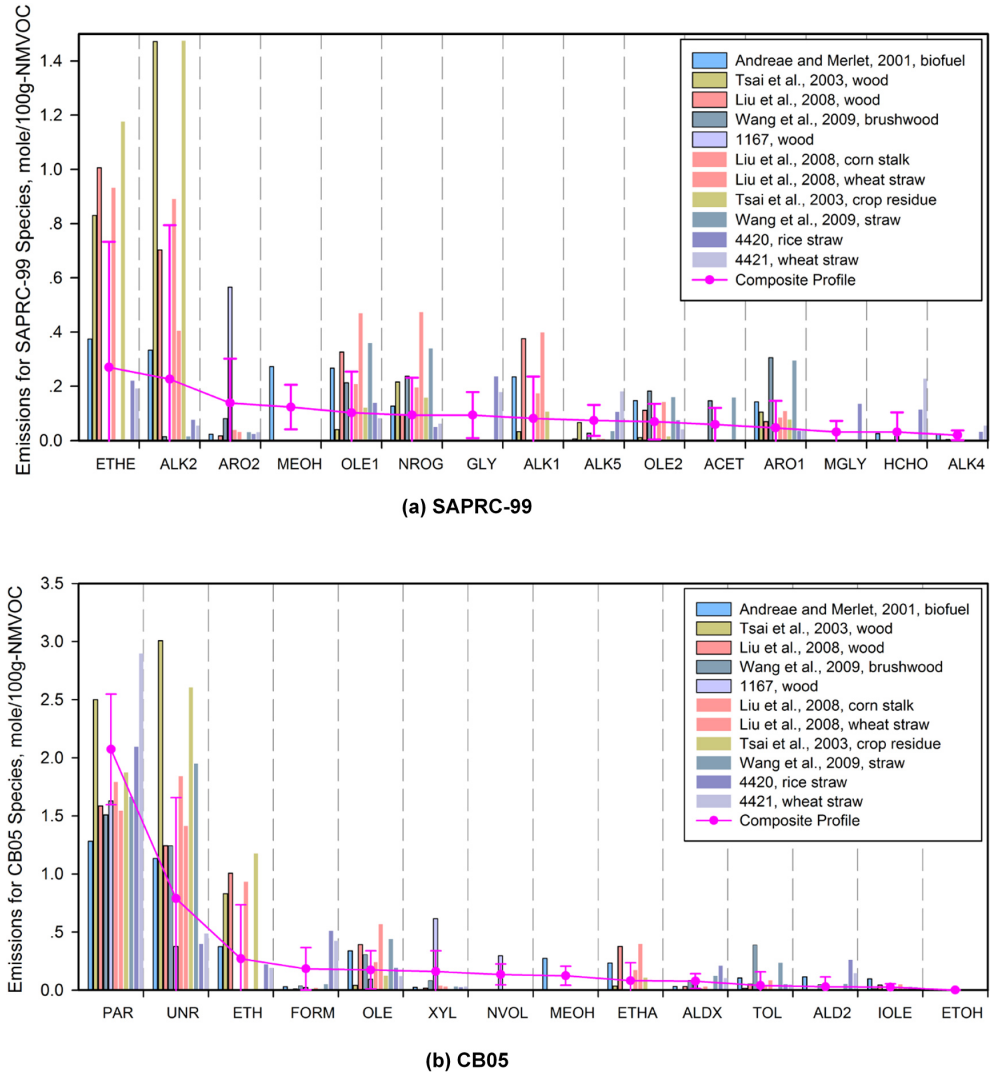

Figure 15. Sensitivity of model-ready emissions to profile selection for the residential biofuel combustion.

difference of OFP between the highest and the lowest values from using different profiles is up to a factor of three, demonstrating the high sensitivity of ozone formation to profiles. The composite profile represents the average level of ozone formation for the biofuel combustion source.

We further compare the emissions of SAPRC-99 and CB05 species estimated with those 11 different profiles and the composite profile, as presented in Fig. 15. It can be seen that the standard deviations are very large for SAPRC-99, especially for ETHE and ALK2, indicating that model simulations configured with SAPRC-99 mechanism would be sensitive to profile selection. On the other hand, the variations in CB05 species are relatively small compared with SAPRC-99 species, which can be explained by the high degree of lumping for CB05.

Sensitivity tests by both speciated emissions and ozone formation for diesel vehicles are also performed, as showed in Figs. S4 and S5, drawing the same conclusion that ozone formation potentials and model-ready emissions are very sensitive to the profile selection and processing. The immediate implication is that using a single profile will introduce large uncertainty into the speciation process, and the composite profile developed in this work can combine the species information from all profiles and represent the average emission characteristics of the emitting source. Thus the uniform profile processing system that groups and aggregates multiple profiles can reduce the uncertainty associated with profile selection, especially when one-to-one mapping of emission source to profile is not feasible due to the different degrees of source specificity.

5 Discussion

In this study, we developed a step-by-step assignment framework to map Asian anthropogenic NMVOC emissions to eight chemical mechanisms used in different CTMs. To our best knowledge, this is the first work providing a model-ready NMVOC emissions database over Asia. Compared to previous work, we used mechanism-specific mapping tables from Carter (2013) to accurately assign individual NMVOC emissions to species groups in different chemical mechanisms, which avoided the uncertainties from the species mapping process. We also compiled "composite" profiles, where more than one profile was available for a given source category, to reduce the uncertainties arising from conflicting individual measurements and the empirical selection of profiles.

Although we believe that the uncertainties in model-ready emissions provided by this work are reduced significantly through our approach, they are still high, mainly due to inadequacies in source profiles. More local measurements with standard source-specific sampling and analysis methods are needed to reduce the discrepancies among different measurements and enhance the data quality of profiles. Another remaining uncertainty in this work is the mismatch between profile and source classification in inventories. The level of detail in source profile measurements is usually higher than that in the source categories of bottom-up inventories. The composite profiles combined from different measurements then imply a hidden assumption that each profile has the same weighting factor in that source category, which is not always true. In future work, more detailed source category classification that balances the complexity and data availability would help to narrow the uncertainties.

Top-down constraints from in situ observations provide useful information for understanding emissions of NMVOC species through correlations between species (e.g., Barletta et al., 2008; Tang et al., 2008; Duncan et al., 2010; Boeke et al., 2011) or source apportionment models (e.g., Liu et al., 2008a, b; Wang et al., 2013). Since profiles are key factors both in receptor models (e.g., the chemical mass balance model) and speciated NMVOC inventory developments, the inconsistency between "receptor-oriented" and "bottom-up" emission estimates may be caused by differences in profile selection to some degree, which needs more analysis in future work. Recent advancements in satellite observations provide additional constraints on NMVOC emissions through formaldehyde and glyoxal column densities (Wittrock et al., 2006; Fu et al., 2007; Liu et al., 2012). Using glyoxal observations from the SCIAMACHY satellite instrument, Liu et al. (2012) concluded that the underestimated aromatics emissions in current inventories are the most likely missing source of glyoxal. From this work, we found that primary emissions of glyoxal from biomass burning might be another important source. Integration of bottom-up inventories and satellite observations would help to close the gap between emission inventories and observations in the future.

The Supplement related to this article is available online at doi:10.5194/acp-14-5617-2014-supplement.

Acknowledgements. The work was supported by China's National Basic Research Program (2010CB951803 and 2014CB441301), the National Science Foundation of China (41222036 and 21221004), and the Tsinghua University Initiative Research Program (2011Z01026). This work was partly sponsored by the US EPA STAR grant R83337601 at Argonne National Laboratory and North Carolina State University.

Edited by: G. Frost

Appendix A

Table A1. Description of SAPRC-99 NMVOC emitting species from anthropogenic sources*.

Species in SAPRC-99	Description
ACET	Acetone
ALK1	Primarily ethane
ALK2	Primarily propane and acetylene
ALK3	Alkanes and other non-aromatic compounds that react only with OH, and have k_{OH} between 2.5×10^3 and 5×10^3 ppm^{-1} min^{-1}
ALK4	Alkanes and other non-aromatic compounds that react only with OH, and have k_{OH} between 5×10^3 and 1×10^4 ppm^{-1} min^{-1}
ALK5	Alkanes and other non-aromatic compounds that react only with OH, and have k_{OH} greater than 1×10^4 ppm^{-1} min^{-1}
ARO1	Aromatics with k_{OH} <2×10^4 ppm^{-1} min^{-1}
ARO2	Aromatics with $k_{OH} > 2 \times 10^4$ ppm^{-1} min^{-1}
BACL	Biacetyl
BALD	Aromatic aldehydes (e.g., benzaldehyde)
CCHO	Methyl Hydroperoxide
CRES	Cresols
ETHE	Ethene
GLY	Glyoxal
HCHO	Formaldehyde
IPRD	Unsaturated aldehydes other than acrolein and methacrolein
MACR	Methacrolein
MEK	Ketones and other non-aldehyde oxygenated products which react with OH radicals slower than 5×10^{-12} cm^3 molec^{-2} s^{-1}
MEOH	Methyl alcohol
MGLY	Methylglyoxal
MVK	Aromatic aldehydes (e.g., benzaldehyde)
NROG	Unreactive organic chemicals
NVOL	Nonvolatile organic chemicals
OLE1	Alkenes (other than ethene) with k_{OH} <7×10^4 ppm^{-1} min^{-1}
OLE2	Alkenes with $k_{OH} > 7 \times 10^4$ ppm^{-1} min^{-1}
PHEN	Phenol
PRD2	Ketones and other non-aldehyde oxygenated products which react with OH radicals faster than 5×10^{-12} cm^3 molec^{-2} s^{-1}
RCHO	Lumped C3$^+$ Aldehydes

* Source: Carter (2000).

Table A2. Description of CB05 NMVOC emitting species from anthropogenic sources*.

Species in CB05	Description
ALD2	Acetaldehyde
ALDX	Propionaldehyde and higher aldehydes
ETH	Ethene
ETHA	Ethane
ETOH	Ethyl alcohol
FORM	Formaldehyde
IOLE	Internal olefin carbon bond (R-C=C-R)
MEOH	Methyl alcohol
NVOL	Nonvolatile organic chemicals
OLE	Terminal olefin carbon bond (R-C=C)
PAR	Paraffin carbon bond (C-C)
TOL	Toluene and other monoalkyl aromatics
UNR	Unreactive VOCs
XYL	Xylene and other polyalkyl aromatics

* Source: http://www.camx.com/files/cb05_final_report_120805.aspx.

Table A3. Description of GEOS-CHEM NMVOC emitting species from anthropogenic sources*.

Species in GEOS-Chem	Description
ACET	Acetone
ALD2	Acetaldehyde
ALK4	Lumped > = C4 Alkanes
C2H6	Ethane
C3H8	Propane
CH2O	Formaldehyde
MEK	Methyl Ethyl Ketone
PRPE	Lumped > = C3 Alkenes

* Source: http://acmg.seas.harvard.edu/geos/doc/man/.

Table A4. Description of MAZART-4 NMVOC emitting species from anthropogenic sources*.

Species for MOZART-4	Description
BIGALK	Lumped alkanes C > 3
BIGENE	Lumped alkenes C > 3
TOLUENE	Lumped aromatics
C3H6	Propene
C3H8	Propane
C2H6	Ethane
C2H4	Ethene
MEK	Methyl ethyl ketone
CH2O	Formaldehyde
CH3CHO	Acetaldehyde
CH3COCH3	Acetone
CH3OH	Methyl alcohol
C2H5OH	Ethyl alcohol

* Source: Emmons et al. (2010).

References

Andreae, M. O. and Merlet, P.: Emission of trace gases and aerosols from biomass burning, Glob. Biogeochem. Cy., 15, 955–966, doi:10.1029/2000GB001382, 2001.

Barletta, B., Meinardi, S., Simpson, I. J., Zou, S., Sherwood Rowland, F., and Blake, D. R.: Ambient mixing ratios of nonmethane hydrocarbons (NMHCs) in two major urban centers of the Pearl River Delta (PRD) region: Guangzhou and Dongguan, Atmos. Environ., 42, 4393–4408, 2008.

Bo, Y., Cai, H., and Xie, S. D.: Spatial and temporal variation of historical anthropogenic NMVOCs emission inventories in China, Atmos. Chem. Phys., 8, 7297–7316, doi:10.5194/acp-8-7297-2008, 2008.

Boeke, N. L., Marshall, J. D., Alvarez, S., Chance, K. V., Fried, A., Kurosu, T. P., Rappengluck, B., Richter, D., Walega, J., Weibring, P., and Millet, D. B.: Formaldehyde columns from the Ozone Monitoring Instrument: Urban versus background levels and evaluation using aircraft data and a global model, J. Geophys. Res., 116, D05303, doi:10.1029/2010JD014870, 2011.

Cai, H. and Xie, S. D.: Tempo-spatial variation of emission inventories of speciated volatile organic compounds from on-road vehicles in China, Atmos. Chem. Phys., 9, 6983–7002, doi:10.5194/acp-9-6983-2009, 2009.

Carlton, A. G., Turpin, B. J., Altieri, K. E., Seitzinger, S., Reff, A., Lim, H.-J., and Ervens, B.: Atmospheric oxalic acid and SOA production from glyoxal: Results of aqueous photooxidation experiments, Atmos. Environ., 41, 7588–7602, 2007.

Carter, W. P. L.: Development of ozone reactivity scales for volatile organic compounds, J. Air Waste Manage., 44, 881–899, 1994.

Carter, W. P. L.: Documentation of the SAPRC-99 chemical mechanism for VOC reactivity assessment, report to the California Air Resources Board, available at: http://www.engr.ucr.edu/~carter/reactdat.htm (last access: October 2013), 2000.

Carter, W. P. L.: Development of the SAPRC-07 chemical mechanism, Atmos. Environ., 44, 5324–5335, 2010.

Carter, W. P. L.: Development of an improved chemical speciation database for processing emissions of volatile organic compounds for air quality models, report available at: http://www.engr.ucr.edu/~carter/emitdb/ (last access: November 2013), 2013.

Christian, T. J., Kleiss, B., Yokelson, R. J., Holzinger, R., Crutzen, P. J., Hao, W. M., Shirai, T., and Blake, D. R.: Comprehensive laboratory measurements of biomass-burning emissions: 2. First intercomparison of open-path FTIR, PTR-MS, and GC-MS/FID/ECD, J. Geophys. Res., 109, D02311, doi:10.1029/2003JD003874, 2004.

Dong, X., Gao, Y., Fu, J. S., Li, J., Huang, K., Zhuang, G., and Zhou, Y.: Probe into gaseous pollution and assessment of air quality benefit under sector dependent emission control strategies over megacities in Yangtze River Delta, China, Atmos. Environ., 79, 841–852, 2013.

Duffy, B. L., Nelson, P. F., Ye, Y., and Weeks, I. A.: Speciated hydrocarbon profiles and calculated reactivities of exhaust and evaporative emissions from 82 in-use light-duty Australian vehicles, Atmos. Environ., 33, 291–307, 1999.

Duncan, B. N., Yoshida, Y., Olson, J. R., Sillman, S., Martin, R. V., Lamsal, L., Hu, Y., Pickering, K. E., Retscher, C., Allen, D. J., and Crawford, J. H.: Application of OMI observations to a space-based indicator of NO_x and VOC controls on surface ozone formation, Atmos. Environ., 44, 2213–2223, 2010.

Emmons, L. K., Walters, S., Hess, P. G., Lamarque, J. F., Pfister, G. G., Fillmore, D., Granier, C., Guenther, A., Kinnison, D., Laepple, T., Orlando, J., Tie, X., Tyndall, G., Wiedinmyer, C., Baughcum, S. L., and Kloster, S.: Description and evaluation of the Model for Ozone and Related chemical Tracers, version 4 (MOZART-4), Geosci. Model Dev., 3, 43–67, doi:10.5194/gmd-3-43-2010, 2010.

Ervens, B. and Volkamer, R.: Glyoxal processing by aerosol multiphase chemistry: towards a kinetic modeling framework of secondary organic aerosol formation in aqueous particles, Atmos. Chem. Phys., 10, 8219–8244, doi:10.5194/acp-10-8219-2010, 2010.

Fu, J. S., Streets, D. G., Jang, C. J., Hao, J. M., He, K. B., Wang, L. T., and Zhang, Q.: Modeling Regional/Urban Ozone and Particulate Matter in Beijing, China, J. Air Waste Manage., 59, 37–44, 2009.

Fu, T. M., Jacob, D. J., Palmer, P. I., Chance, K., Wang, Y. X. X., Barletta, B., Blake, D. R., Stanton, J. C., and Pilling, M. J.: Space-based formaldehyde measurements as constraints on volatile organic compound emissions in east and south Asia and implications for ozone, J. Geophys. Res., 112, D06312, doi:10.1029/2006JD007853, 2007.

Fu, T.-M., Jacob D. J., Wittrock, F., Burrows, J. P., Vrekoussis, M., and Henze, D. K.: Global budgets of atmospheric glyoxal and methylglyoxal, and implications for formation of secondary organic aerosols, J. Geophys. Res., 113, D15303, doi:10.1026/2007JD009505, 2008.

Gery, M. W., Whitten, G. Z., Killus, J. P., and Dodge, M. C.: A photochemical kinetics mechanism for urban and regional scale computer modeling, J. Geophys. Res., 94, 12925–12956, doi:10.1029/JD094iD10p12925, 1989.

Goliff, W. S., Stockwell, W. R., and Lawson, C. V.: The regional atmospheric chemistry mechanism, version 2, Atmos. Environ., 68, 174–185, 2013.

Guenther, A. B., Jiang, X., Heald, C. L., Sakulyanontvittaya, T., Duhl, T., Emmons, L. K., and Wang, X.: The Model of Emissions of Gases and Aerosols from Nature version 2.1 (MEGAN2.1): an extended and updated framework for modeling biogenic emissions, Geosci. Model Dev., 5, 1471–1492, doi:10.5194/gmd-5-1471-2012, 2012.

Hogrefe, C., Lynn, B., Civerolo, K., Ku, J. Y., Rosenthal, J., Rosenzweig, C., Goldberg, R., Gaffin, S., Knowlton, K., and Kinney, P. L.: Simulating changes in regional air pollution over the eastern United States due to changes in global and regional climate and emissions, J. Geophys. Res., 109, D22301, doi:10.1029/2004jd004690, 2004.

Hopkins, J. R., Lewis, A. C., and Read, K. A.: A two-column method for long-term monitoring of non-methane hydrocarbons (NMHCs) and oxygenated volatile organic compounds (oVOCs), J. Environ. Monitor., 5, 8–13, doi:10.1039/b202798d, 2003.

Houyoux, M. R., Vukovich, J. M., Coats, C. J., Wheeler, N. J. M., and Kasibhatla, P. S.: Emission inventory development and processing for the Seasonal Model for Regional Air Quality (SMRAQ) project, J. Geophys. Res., 105, 9079–9090, 2000.

Hsu, Y. and Divita, F.: SPECIATE 4.2, speciation database development documentation, final report, EPA/600-R-09/-38, 2009.

Huang, Y., Ho, S. S. H., Ho, K. F., Lee, S. C., Yu, J. Z., and Louie, P. K. K.: Characteristics and health impacts of VOCs and carbonyls

associated with residential cooking activities in Hong Kong, J. Hazard. Mater., 186, 344–351, 2011.

Kelly, T. J. and Holdren, M. W.: Applicability of canisters for sample storage in the determination of hazardous air pollutants, Atmos. Environ., 29, 2595–2608, 1995.

Klimont, Z., Streets, D. G., Gupta, S., Cofala, J., Fu, L. X., and Ichikawa, Y.: Anthropogenic emissions of non-methane volatile organic compounds in China, Atmos. Environ., 36, 1309–1322, 2002.

Kurokawa, J., Ohara, T., Morikawa, T., Hanayama, S., Janssens-Maenhout, G., Fukui, T., Kawashima, K., and Akimoto, H.: Emissions of air pollutants and greenhouse gases over Asian regions during 2000–2008: Regional Emission inventory in ASia (REAS) version 2, Atmos. Chem. Phys., 13, 11019–11058, doi:10.5194/acp-13-11019-2013, 2013.

Lai, C. H., Chang, C. C., Wang, C. H., Shao, M., Zhang, Y. H., and Wang, J. L.: Emissions of liquefied petroleum gas (LPG) from motor vehicles, Atmos. Environ., 43, 1456–1463, 2009.

Lamarque, J.-F., Bond, T. C., Eyring, V., Granier, C., Heil, A., Klimont, Z., Lee, D., Liousse, C., Mieville, A., Owen, B., Schultz, M. G., Shindell, D., Smith, S. J., Stehfest, E., Van Aardenne, J., Cooper, O. R., Kainuma, M., Mahowald, N., McConnell, J. R., Naik, V., Riahi, K., and van Vuuren, D. P.: Historical (1850–2000) gridded anthropogenic and biomass burning emissions of reactive gases and aerosols: methodology and application, Atmos. Chem. Phys., 10, 7017–7039, doi:10.5194/acp-10-7017-2010, 2010.

Lin, M., Fiore, A. M., Horowitz, L. W., Cooper, O. R., Naik, V., Holloway, J., Johnson, B. J., Middlebrook, A. M., Oltmans, S. J., Pollack, I. B., Ryerson, T. B., Warner, J. X., Wiedinmyer, C., Wilson, J., and Wyman, B.: Transport of Asian ozone pollution into surface air over the western United States in spring, J. Geophys. Res., 117, D00V07, doi:10.1029/2011JD016961, 2012.

Liu, Y., Shao, M., Fu, L. L., Lu, S. H., Zeng, L. M., and Tang, D. G.: Source profiles of volatile organic compounds (VOCs) measured in China: Part I, Atmos. Environ., 42, 6247–6260, 2008a.

Liu, Y., Shao, M., Lu, S., Chang, C.-C., Wang, J.-L., and Fu, L.: Source apportionment of ambient volatile organic compounds in the Pearl River Delta, China: Part II, Atmos. Environ., 42, 6261–6274, 2008b.

Liu, Z., Wang, Y., Vrekoussis, M., Richter, A., Wittrock, F., Burrows, J. P., Shao, M., Chang, C.-C., Liu, S.-C., Wang, H., and Chen, C.: Exploring the missing source of glyoxal (CHOCHO) over China, Geophys. Res. Lett., 39, L10812, doi:10.1029/2012GL051645, 2012.

Na, K., Kim, Y. P., Moon, I., and Moon, K. C.: Chemical composition of major VOC emission sources in the Seoul atmosphere, Chemosphere, 55, 585–594, 2004.

Ohara, T., Akimoto, H., Kurokawa, J., Horii, N., Yamaji, K., Yan, X., and Hayasaka, T.: An Asian emission inventory of anthropogenic emission sources for the period 1980–2020, Atmos. Chem. Phys., 7, 4419–4444, doi:10.5194/acp-7-4419-2007, 2007.

Piccot, S. D., Watson, J. J., and Jones, J. W.: A global inventory of volatile organic compound emissions from anthropogenic sources, J. Geophys. Res., 97, 9897–9912, 1992.

Reff, A., Bhave, P. V., Simon, H., Pace, T. G., Pouliot, G. A., Mobley, J. D., and Houyoux, M.: Emissions Inventory of $PM_{2.5}$ Trace Elements across the United States, Environ. Sci. Technol., 43, 5790–5796, 2009.

Schauer, J. J., Kleeman, M. J., Cass, G. R., and Simoneit, B. R. T.: Measurement of emissions from air pollution sources. 2. C-1 through C-30 organic compounds from medium duty diesel trucks, Environ. Sci. Technol., 33, 1578–1587, 1999.

Schauer, J. J., Kleeman, M. J., Cass, G. R., and Simoneit, B. R. T.: Measurement of emissions from air pollution sources. 3. C-1-C-29 organic compounds from fireplace combustion of wood, Environ. Sci. Technol., 35, 1716–1728, 2001.

Schauer, J. J., Kleeman, M. J., Cass, G. R., and Simoneit, B. R. T.: Measurement of emissions from air pollution sources. 5. C-1-C-32 organic compounds from gasoline-powered motor vehicles, Environ. Sci. Technol., 36, 1169–1180, 2002.

Simon, H., Beck, L., Bhave, P. V., Divita, F., Hsu, Y., Luecken, D., Mobley, J. D., Pouliot, G. A., Reff, A., Sarwar, G., and Strum, M.: The development and uses of EPA's SPECIATE database, Atmos. Pollut. Res., 1, 196–206, 2010.

Song, Y., Shao, M., Liu, Y., Lu, S., Kuster, W., Goldan, P., and Xie, S.: Source Apportionment of Ambient Volatile Organic Compounds in Beijing, Environ. Sci. Technol., 41, 4348–4353, 2007.

Stockwell W. R., Middleton, P., Chang, J. S., and Tang, X.: The second generation Regional Acid Deposition Model chemical mechanism for regional air quality modeling, J. Geophys. Res., 95, 16343–16367, 1990.

Stockwell, W. R., Kirchner, F., Kuhn, M., and Seefeld, S.: A new mechanism for regional atmospheric chemistry modeling, J. Geophys. Res., 102, 25847–25879, 1997.

Streets, D. G., Bond, T. C., Carmichael, G. R., Fernandes, S. D., Fu, Q., He, D., Klimont, Z., Nelson, S. M., Tsai, N. Y., Wang, M. Q., Woo, J. H., and Yarber, K. F.: An inventory of gaseous and primary aerosol emissions in Asia in the year 2000, J. Geophys. Res., 108, 8809, doi:10.1029/2002JD003093, 2003.

Tang, J. H., Chan, L. Y., Chan, C. Y., Li, Y. S., Chang, C. C., Wang, X. M., Zou, S. C., Barletta, B., Blake, D. R., and Wu, D.: Implications of changing urban and rural emissions on non-methane hydrocarbons in the Pearl River Delta region of China, Atmos. Environ., 42, 3780–3794, 2008.

Tsai, S. M., Zhang, J. F., Smith, K. R., Ma, Y. Q., Rasmussen, R. A., and Khalil, M. A. K.: Characterization of non-methane hydrocarbons emitted from various cookstoves used in China, Environ. Sci. Technol., 37, 2869–2877, 2003.

US EPA: Guidance on the use of models and other analyses for demonstrating attainment of air quality for ozone, $PM_{2.5}$ and regional haze, US Environmental Protection Agency, United States, 253 pp., 2007.

van der Werf, G. R., Randerson, J. T., Giglio, L., Collatz, G. J., Mu, M., Kasibhatla, P. S., Morton, D. C., DeFries, R. S., Jin, Y., and van Leeuwen, T. T.: Global fire emissions and the contribution of deforestation, savanna, forest, agricultural, and peat fires (1997–2009), Atmos. Chem. Phys., 10, 11707–11735, doi:10.5194/acp-11707-2010, 2010.

Wang, L., Jang, C., Zhang, Y., Wang, K., Zhang, Q., Streets, D., Fu, J., Lei, Y., Schreifels, J., He, K., Hao, J., Lam, Y.-F., Lin, J., Meskhidze, N., Voorhees, S., Evarts, D., and Phillips, S.: Assessment of air quality benefits from national air pollution control policies in China. Part II: Evaluation of air quality predictions and air quality benefits assessment, Atmos. Environ., 44, 3449–3457, 2010.

Wang, M., Shao, M., Chen, W., Yuan, B., Lu, S., Zhang, Q., Zeng, L., and Wang, Q.: Validation of emission inventories by measurements of ambient volatile organic compounds in Beijing, China, Atmos. Chem. Phys. Discuss., 13, 26933–26979, doi:10.5194/acpd-13-26933-2013, 2013.

Wang, S., Wei, W., Du, L., Li, G., and Hao, J.: Characteristics of gaseous pollutants from biofuel-stoves in rural China, Atmos. Environ., 43, 4148–4154, 2009.

Wang, Y., Zhang, Y., Hao, J., and Luo, M.: Seasonal and spatial variability of surface ozone over China: contributions from background and domestic pollution, Atmos. Chem. Phys., 11, 3511–3525, doi:10.5194/acp-11-3511-2011, 2011.

Wei, W., Wang, S. X., Chatani, S., Klimont, Z., Cofala, J., and Hao, J. M.: Emission and speciation of non-methane volatile organic compounds from anthropogenic sources in China, Atmos. Environ., 42, 4976–4988, 2008.

Wittrock, F., Richter, A., Oetjen, H., Burrows, J. P., Kanakidou, M., Myriokefalitakis, S., Volkamer, R., Beirle, S., Platt, U., and Wagner, T.: Simultaneous global observations of glyoxal and formaldehyde from space, Geophys. Res. Lett., 33, L16804, doi:10.1029/2006GL026310, 2006.

Woo, J. H., Baek, J. M., Kim, J. W., Carmichael, G. R., Thongboonchoo, N., Kim, S. T., and An, J. H.: Development of a multi-resolution emission inventory and its impact on sulfur distribution for Northeast Asia, Water Air Soil Poll., 148, 259–278, 2003.

Xing, J., Zhang, Y., Wang, S., Liu, X., Cheng, S., Zhang, Q., Chen, Y., Streets, D. G., Jang, C., Hao, J., and Wang, W.: Modeling study on the air quality impacts from emission reductions and atypical meteorological conditions during the 2008 Beijing Olympics, Atmos. Environ., 45, 1786–1798, 2011.

Yarwood, G., Rao, S., Yocke, M., and Whitten, G.: Updates to the Carbon Bond Chemical Mechanism: CB05, Final Report to the US EPA, RT-0400675, available at: http://www.camx.com (last access: October 2013), 2005.

Yuan, B., Shao, M., Lu, S., and Wang, B.: Source profiles of volatile organic compounds associated with solvent use in Beijing, China, Atmos. Environ., 44, 1919–1926, 2010.

Zaveri, R. A. and Peters, L. K.: A new lumped structure photochemical mechanism for large-scale applications, J. Geophys. Res., 104, 30387–30415, doi:10.1029/1999JD900876, 1999.

Zhang, Q., Streets, D. G., Carmichael, G. R., He, K. B., Huo, H., Kannari, A., Klimont, Z., Park, I. S., Reddy, S., Fu, J. S., Chen, D., Duan, L., Lei, Y., Wang, L. T., and Yao, Z. L.: Asian emissions in 2006 for the NASA INTEX-B mission, Atmos. Chem. Phys., 9, 5131–5153, doi:10.5194/acp-9-5131-2009, 2009.

Zhang, Y., Liu, X.-H., Olsen, K. M., Wang, W.-X., Do, B. A., and Bridgers, G. M.: Responses of future air quality to emission controls over North Carolina, Part II: Analyses of future-year predictions and their policy implications, Atmos. Environ., 44, 2767–2779, 2010.

Zhang, Y., Chen, Y., Sarwar, G., and Schere, K.: Impact of gas-phase mechanisms on Weather Research Forecasting Model with Chemistry (WRF/Chem) predictions: Mechanism implementation and comparative evaluation, J. Geophys. Res., 117, D01301, doi:10.1029/2011JD015775, 2012.

Zhang, Y., Wang, W., Wu, S.-Y., Kang, K., Minoura, H., and Wang, Z.-F.: Impacts of updated emission inventories on source apportionment of fine particle and ozone over the southeastern US, Atmos. Environ., 88, 133–154, doi:10.1016/j.atmosenv.2014.01.035, 2014.

Zhang, Y. L., Wang, X. M., Zhang, Z., Lu S. J., Shao, M., Lee, F. S. C., and Yu, J. Z.: Species profiles and normalized reactivity of volatile organic compounds from gasoline evaporation in China, Atmos. Environ., 79, 110–118, 2013.

Zhao, Y., Nielsen, C. P., Lei, Y., McElroy, M. B., and Hao, J.: Quantifying the uncertainties of a bottom-up emission inventory of anthropogenic atmospheric pollutants in China, Atmos. Chem. Phys., 11, 2295–2308, doi:10.5194/acp-11-2295-2011, 2011.

Zheng, J. Y., Shao, M., Che, W. W., Zhang, L. J., Zhong, L. J., Zhang, Y. H., and Streets, D.: Speciated VOC Emission Inventory and Spatial Patterns of Ozone Formation Potential in the Pearl River Delta, China, Environ. Sci. Technol., 43, 8580–8586, 2009.